

RESEARCH ARTICLE

Improving the Molecular Ion Signal Intensity for In Situ Liquid SIMS Analysis

Yufan Zhou,^{1,2} Juan Yao,³ Yuanzhao Ding,^{3,4} Jiachao Yu,³ Xin Hua,³ James E. Evans,² Xiaofei Yu,^{1,2} David B. Lao,⁵ David J. Heldebrant,⁵ Satish K. Nune,⁵ Bin Cao,⁴ Mark E. Bowden,² Xiao-Ying Yu,³ Xue-Lin Wang,¹ Zihua Zhu² 

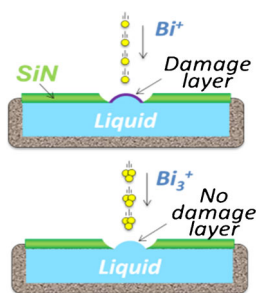
¹School of Physics, State Key Laboratory of Crystal Materials and Key Laboratory of Particle Physics and Particle Irradiation (MOE), Shandong University, Jinan, 250100, China

²W. R. Wiley Environmental Molecular Sciences Laboratory, Earth and Biological Sciences Directorate, Pacific Northwest National Laboratory, Richland, WA 99354, USA

³Earth and Biological Sciences Directorate, Pacific Northwest National Laboratory, Richland, WA 99354, USA

⁴School of Civil and Environmental Engineering and Singapore Centre for Environmental Life Sciences Engineering, Nanyang Technological University, Singapore, 639798, Singapore

⁵Energy and Environment Directorate, Pacific Northwest National Laboratory, Richland, WA 99354, USA



Abstract. In situ liquid secondary ion mass spectrometry (SIMS) enabled by system for analysis at the liquid vacuum interface (SALVI) has proven to be a promising new tool to provide molecular information at solid–liquid and liquid–vacuum interfaces. However, the initial data showed that useful signals in positive ion spectra are too weak to be meaningful in most cases. In addition, it is difficult to obtain strong negative molecular ion signals when $m/z > 200$. These two drawbacks have been the biggest obstacle towards practical use of this new analytical approach. In this study, we report that strong and reliable positive and negative molecular signals are achievable after optimizing the SIMS experimental conditions. Four model systems, including a 1,8-diazabicycloundec-7-ene (DBU)-base switchable ionic liquid, a live

Shewanella oneidensis biofilm, a hydrated mammalian epithelia cell, and an electrolyte popularly used in Li ion batteries were studied. A signal enhancement of about two orders of magnitude was obtained in comparison with non-optimized conditions. Therefore, molecular ion signal intensity has become very acceptable for use of in situ liquid SIMS to study solid–liquid and liquid–vacuum interfaces.

Keywords: In situ liquid SIMS, Solid–liquid interface, Molecular imaging, Ionic liquid, Biofilm, Cell, Electrolyte

Received: 17 April 2016/Revised: 8 August 2016/Accepted: 10 August 2016/Published Online: 6 September 2016

Introduction

Ionic and molecular distribution and transport at solid–liquid and gas–liquid interfaces are of great interest in many fields. However, such information has been difficult to obtain because of the lack of desirable in situ analysis tools. At biointerfaces, for instance, the distribution of small functional ions such as

Na^+ , K^+ , Ca^{2+} , or small organic molecules such as glucose and phospholipid molecules remains unclear. This is despite the use of many in situ techniques such as atomic force microscopy [1, 2], fluorescence [3, 4], Raman [5], infrared [6, 7], and surface plasmon resonance [8].

Secondary ion mass spectrometry (SIMS) is a very powerful surface analysis tool. It can provide elemental, isotopic, and molecular information with high sensitivity (ppb to ppm level) and good spatial resolution (down to sub-nm in depth resolution and ~ 50 nm in lateral resolution) [9, 10]. However, as a high vacuum technique, it has been traditionally used to analyze solid samples. In situ liquid SIMS was developed in the last several years and one of its unique capabilities is the analysis of liquid–solid and liquid–vacuum interfaces

Electronic supplementary material The online version of this article (doi:10.1007/s13361-016-1478-x) contains supplementary material, which is available to authorized users.

Correspondence to: Zihua Zhu; e-mail: zihua.zhu@pnl.gov, Xue-Lin Wang; e-mail: xuelinwang@sdu.edu.cn, Xiao-Ying Yu; e-mail: xiaoying.yu@pnl.gov

[11–18]. To enable in situ liquid SIMS measurement, a vacuum-compatible device named system for analysis at the liquid–vacuum interface (SALVI) was developed [11, 12], where a liquid of interest can be sealed in a microfluidic channel under a thin (e.g., 100 nm) silicon nitride (SiN) membrane. The key to in situ liquid SIMS measurements is the use of a ~ 2 μm diameter aperture on the thin SiN membrane, through which the liquid interface and the liquid itself can be analyzed. Because the aperture size is small, surface tension can hold the liquid beneath the SiN membrane, and the evaporation of the liquid from the aperture does not cause any unacceptable problem to the vacuum system of the SIMS instrument [12]. The SiN membrane surface can be modified and the liquid in the cell can be changed, allowing various liquid–solid interfaces to be studied. As a result, in situ liquid SIMS has been successfully applied to analysis of live biofilms [16, 17], protein-modified Au nanoparticles [13], electrochemical reactions [15, 19], and the formation of solid–electrolyte interface in a Li-ion battery [18].

However, initial studies reported detection of only negative molecular ions [11–17] because the signals of the positive ion spectra were too weak to be meaningful. In addition, although negative molecular ions could be successfully analyzed, their signal intensity was not strong [16, 17]. Therefore, the SIMS community has some genuine concern for using this new innovation for further practical applications.

In this work, we report an enhancement of two orders of magnitude in molecular signal intensity by using a cluster primary ion beam with reasonable currents. Both positive and negative molecular ion signals can be readily detected so that signal intensity will no longer be a major concern in in situ SIMS analysis. Four model systems, comprising a 1,8-diazabicyclo[5.4.0]undec-7-ene (DBU)-base switchable ionic liquid [20], a live *Shewanella oneidensis* biofilm [21], a hydrated mammalian cell, and a LiPF_6 electrolyte [18] were studied.

Experimental

SALVI Fabrication

The details of SALVI fabrication have been extensively described in our previous publications [11, 12, 16]. In brief, a microfluidic channel with a cross-section of 200×300 μm^2 was prepared on a PDMS block. A 100 nm thick SiN membrane with a window size of 1.5×1.5 mm^2 supported on a 7.5×7.5 mm^2 silicon wafer was bonded to the PDMS block with the microfluidic channel located at the center of the SiN window. The liquid was introduced into the microfluidic channel through PTFE tubes, and the two ends of the PTFE tubes were sealed by a union [22]. The sealed SALVI device was loaded on a sample holder prior to ToF-SIMS analysis.

Sample Preparation

The DBU was ordered from Sigma Aldrich (St. Louis, MO, USA) and distilled over sodium before transfer to a nitrogen-filled glovebox. Anhydrous 1-hexanol ($\geq 99.5\%$) was purchased from Acros (Pittsburg, PA, USA) and used without any further treatment. DBU and 1-hexanol were mixed in a 1:1 molar ratio and sealed in a high-pressure Parr reactor inside of a nitrogen-filled glovebox. The reactor was pressurized to 3–4 bar of CO_2 and stirred for 16 h for complete conversion to the ionic liquid. The reactor was then vented, opened at ambient condition, and the ionic liquid was immediately introduced into a SALVI device for ToF-SIMS analysis. It should be noted that many ionic liquids have very low vapor pressure and they can be directly analyzed using regular ToF-SIMS [23–26]. The DBU-base switchable ionic liquid is unique because it decomposes to release CO_2 under vacuum (as shown in Scheme 1 [20]). Therefore, it must be loaded in SALVI before it can be analyzed by ToF-SIMS.

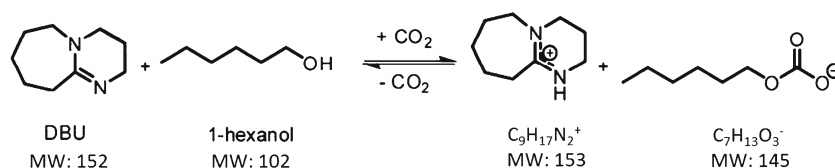
The biofilm culture followed the description in our previous papers [16, 17, 21]. In brief, the *Shewanella oneidensis* MR-1 was grown overnight in the MM1 medium at 30 °C. After the SALVI microfluidic device was sterilized by 70% ethanol, the diluted culture was inoculated into the microchannel. After inoculation, the flow was stopped in 4 h to facilitate the bacteria cells' initial attachment. Afterwards, MM1 medium was continuously supplied for biofilm growth. After ~ 7 d, sufficient biofilm was formed in the microchannel, which was confirmed by fluorescence analysis. The SALVI device was then disconnected from the supply of the MM1 medium and sealed for immediate ToF-SIMS analysis.

The mammalian cells used in this research were alveolar type II epithelial mouse lung C10 cells. The details of C10 cell culturing in SALVI have been described in our previous paper [27]. In brief, after being thoroughly washed by 70% ethanol and sterilized DI water, the microchannel was treated with 10 mg mL^{-1} fibronectin solution overnight. Subsequently, 500 μL C10 cell suspension (the concentration is about 1×10^6 cells per mL) was injected into the microchannel, and then incubated at 37 °C for 1 d. Fresh medium was applied for the following 2-d cell culturing. Then the cultured cells were washed with PBS and fixed with 4% paraformaldehyde. DI water was introduced into the channel after the cells were fixed before ToF-SIMS analysis in order to reduce the interference signals from the PBS during the ToF-SIMS analysis.

A battery grade electrolyte, composed of 1.0 M LiPF_6 in ethylene carbonate (EC) and dimethyl carbonate (DMC) (EC:DMC=1:2, volume ratio), was purchased from Sigma Aldrich (St. Louis, MO, USA) and directly used for ToF-SIMS analysis without any further treatment.

Instrumentation

ToF-SIMS measurements were performed on a TOF.SIMS5-100 instrument (IONTOF GmbH, Münster, Germany) in the environmental molecular sciences laboratory (EMSL) located at Pacific Northwest National Laboratory (PNNL). It was equipped with a 25 kV Bi cluster ion source. In this study,



Scheme 1. Known chemistry of a switchable ionic liquid consisting of DBU, 1-hexanol, and CO₂ [20]

three analysis beams, Bi⁺, Bi₃⁺, and Bi₃⁺⁺, were compared because they could provide reasonable beam currents [28–30]. Focus sizes, currents, and pulse widths of Bi⁺, Bi₃⁺, and Bi₃⁺⁺ beams that were used in this study are listed in Table 1. During in situ liquid SIMS measurement, the analysis beam was focused to submicron size and scanned on a round area with a diameter of about 2 μm to drill an aperture through the SiN membrane. Secondary ion mass spectra, depth profiles, and images were collected simultaneously (as shown in Figure 1). As soon as the SiN membrane was perforated, the characteristic ion signals from the liquid could be observed. If necessary, after the signals from liquids became stable, the pulse width of the analysis beam could be narrowed down from 150–250 ns to 50–80 ns to acquire a better mass resolution mass spectrum to facilitate assignment of high mass ($m/z > 200$) signals [27]. Each measurement was completed after a spectrum of desirable quality was collected (typically 50–400 s after drilling through the SiN membrane). A flood gun with low energy (<10 eV) electrons was used for charge compensation for all measurement. In addition, it was observed that the signal intensity could be further improved if a 1.0 keV O₂⁺ beam with a few nA (<5 nA) current was scanned on a 500 × 500 μm² area around the aperture during data collection.

A high beam current can be obtained if compromising beam focus. The principle is shown in Supplementary Figure S1. One could use the Lens Source to focus the most emission current onto the sample surface; however, the focus was poor (Supplementary Figure S1a). Alternatively, one could defocus the beam using the Lens Source and only allow a small angle of the emission current to pass through Aperture 1 before focusing it onto the sample surface. In this case, the focus is improved (Supplementary Figure S1b) with a low current. Roughly, the beam current on the sample surface was proportional to the square of the optimum beam diameter value. In this research, three diameters were used: 200, 500, and 650 nm. In addition, it was also possible to adjust the beam current by varying the

pulse widths. Owing to the time-of-flight mass selection principle of the Bi source (as shown in Flash S1 in Supplementary Materials), for each ionic species there was a maximum pulse width over which interference from other ion species appeared. For the Bi⁺, Bi₃⁺, and Bi₃⁺⁺ beams (25 kV acceleration), the maximum pulse widths were ~280, ~160, and ~250 ns, respectively. It should be noted that the pulse widths used in this study were narrower than the maximum values. The beam sizes, pulse widths, as well as corresponding DC and pulsed beam currents, are listed in Table 1. A repeat rate of 10 kHz (cycle time = 100 μs) was used and the effective mass range was about m/z 0–800. For readers' convenience, we have used beam size, pulsed current, and ionic species to describe a beam condition (e.g., a 500 nm 0.36 pA Bi₃⁺ beam, or more briefly, a 500 nm Bi₃⁺ beam).

Table 1. Beam Currents and Pulse Widths of Bi⁺, Bi₃⁺, and Bi₃⁺⁺ Beams Used in This Study

Probe size (nm)	DC beam current (pA)	Pulsed current (pA) @ 10 kHz with maximum pulsed width			Pulsed current (pA) used in this research @ 10 kHz and corresponding pulsed width		
		Bi ⁺	Bi ₃ ⁺	Bi ₃ ⁺⁺	Bi ⁺	Bi ₃ ⁺	Bi ₃ ⁺⁺
~200	200	0.29	0.063	0.07	0.2	0.06	0.07
~500	1200	1.72	0.38	0.42	1.2	0.36	0.42
~650	2000	2.87	0.63	0.70	2.0	0.60	0.70
Pulse width (ns)		280 ns	160 ns	252 ns	200 ns	150 ns	250 ns

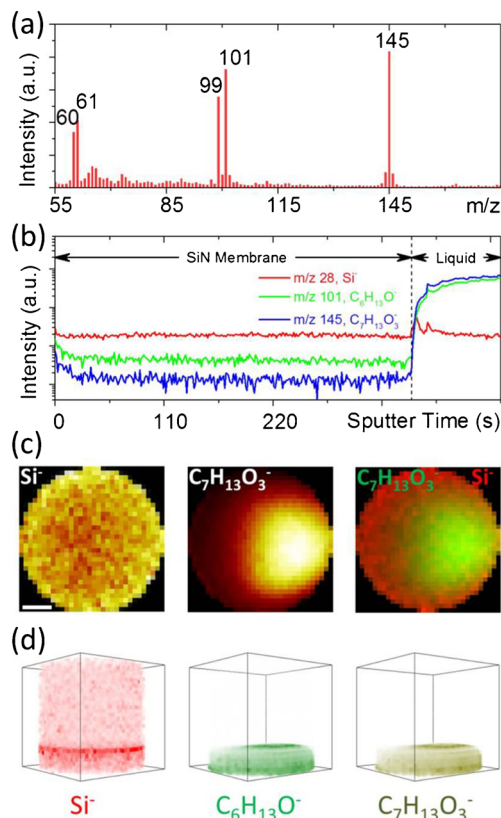


Figure 1. A typical in situ liquid SIMS measurement of the DBU-base ionic liquid sample using a Bi₃⁺ primary ion beam. (a) A negative ion mass spectrum, (b) depth profiles of three representative signals, (c) two-dimensional (2-D) ion images, and (d) three-dimensional (3-D) reconstruction. The scale bar in (c) is equal to 400 nm. Assignment of the major peaks in the spectrum can be seen in Table 2. The m/z 145 peak ($C_7H_{13}O_3^-$) is the molecular ion signal

Table 2. Assignment of Several Representative Negative Ion Signals of the DBU-Base Ionic Liquid

m/z	Formula	Note
60	$\text{CO}_3^-/\text{SiO}_2^-$	Ionic liquid, characteristic fragment ion/SiN membrane
61	HCO_3^-	Ionic liquid, characteristic fragment ion
99	$\text{C}_6\text{H}_{11}\text{O}^- (\text{CH}_3-(\text{CH}_2)_3-\text{CH}=\text{CH}-\text{O}^-)$	1-Hexanol, characteristic fragment ion
101	$\text{C}_6\text{H}_{13}\text{O}^- (\text{CH}_3-(\text{CH}_2)_5-\text{O}^-)$	1-Hexanol, molecular ion
145	$\text{C}_7\text{H}_{13}\text{O}_3^- (\text{CH}_3-(\text{CH}_2)_5-\text{O}-\text{CO}_2^-)$	Ionic liquid, molecular ion

An optical microscope (Olympus BX60, with a 100X objective (NA = 0.80), Center Valley, PA, USA) and a scanning electron microscope (SEM) (Hitachi TM-1000, Tarrytown, NY, USA) were used to determine the size of the apertures on SiN membranes. The optical images were measured as soon as the device was taken out of the SIMS instrument. A thin layer of Au (~10 nm) was deposited on the SiN membrane surface before SEM measurement.

Results and Discussion

Beam Damage Evaluation

In most of our previous studies, a 25 keV Bi^+ beam was used as the primary ion beam, and the beam size was focused to ~200 nm diameter with a current of 0.2–1.0 pA [11, 13–15]. The Bi^+ beam was chosen because it was the most abundant primary ion species, and it could provide the highest current with our instrument (IONTOF V) [29, 30]. In addition, it had been expected that the liquid interface should be self-renewable due to liquid diffusion, and the beam damage of Bi^+ might not be problematic [12].

The DBU-based ionic liquid was used as a model system to evaluate beam damage for two main reasons. First, the chemical components of this system are simple, and secondly it provides very strong molecular ion signals due to its ionic nature. Figure 2 shows the depth profiles of negative molecular ion ($\text{C}_7\text{H}_{13}\text{O}_3^-$) using Bi^+ , Bi_3^+ , and Bi_3^{++} beams. A strong $\text{C}_7\text{H}_{13}\text{O}_3^-$ signal appeared as soon as the Bi_3^+ and Bi_3^{++} beams sputtered through the SiN membrane. The $\text{C}_7\text{H}_{13}\text{O}_3^-$ signal gradually increased and a relatively stable state was reached. By comparison, the $\text{C}_7\text{H}_{13}\text{O}_3^-$ signal was

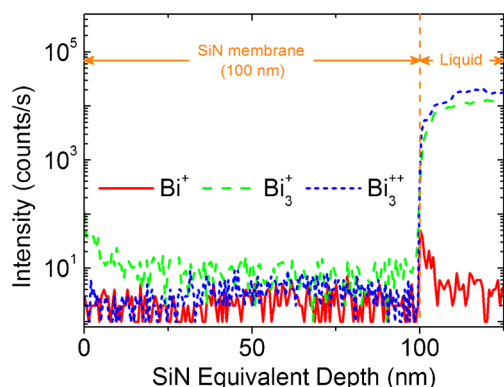


Figure 2. Depth profiles of the $\text{C}_7\text{H}_{13}\text{O}_3^-$ signal in the DBU-base ionic liquid using 500 nm Bi^+ , Bi_3^+ , and Bi_3^{++} beams

very weak when using Bi^+ sputtering. In addition, Figure 3 shows the negative ion spectra of the ionic liquid induced by Bi^+ , Bi_3^+ , and Bi_3^{++} beams. Not only the $\text{C}_7\text{H}_{13}\text{O}_3^-$ signal but also other characteristic signals (e.g., HCO_3^- , $\text{C}_6\text{H}_{11}\text{O}^-$, and $\text{C}_6\text{H}_{13}\text{O}^-$), were weaker when using the Bi^+ beam compared with the Bi_3^+ and Bi_3^{++} beams. This observation suggests that the Bi^+ -induced damage cannot be compensated by the self-renewable rate of the ionic liquid, whereas the Bi_3^+ and Bi_3^{++} -induced beam damage can be effectively compensated. This observation can be explained by high sputter yields of cluster incident ions. The metal cluster incident ions are well-known to provide much higher sputter yields (about one to two orders of magnitude) than the corresponding monatomic incident ions [31–33], and the higher sputter yields of the cluster incident ions can more effectively remove the damaged layer at the sputter interface.

The positive secondary ion spectra showed similar results (i.e., Bi^+ induces significant damage) but Bi_3^+ and Bi_3^{++} can

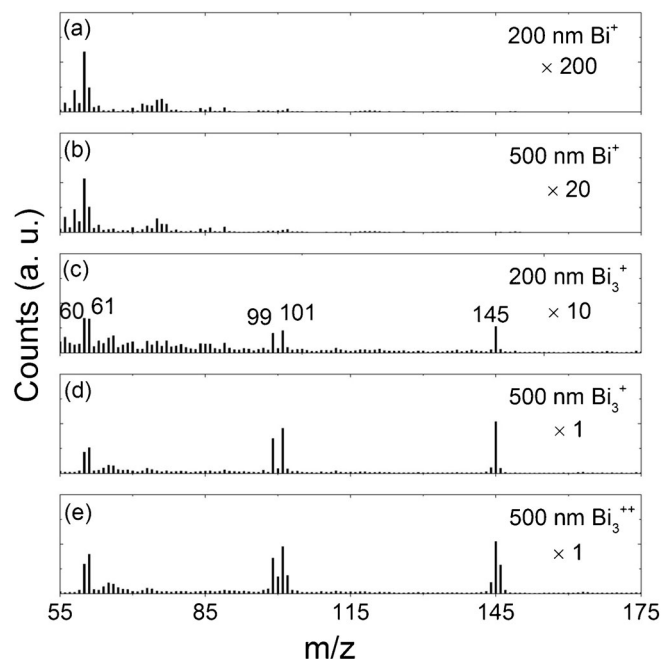


Figure 3. A comparison of negative ion mass spectra of the DBU-base ionic liquid sample using different beam conditions. The m/z 60, 61, 99, 101, and 145 peaks are characteristic peaks of the ionic liquid. The peak assignments can be seen in Table 2. The relatively strong peak 100, 102, and 146 peaks in the spectrum of 500 nm Bi_3^{++} result from wide pulse width of the Bi_3^{++} beam. The spectra induced by 650 nm Bi^+ , Bi_3^+ , and Bi_3^{++} beams are not shown because they lead to liquid leaking easily

provide strong and stable molecular ion signals (Supplementary Figure S2). Apparently, using cluster primary ions is the key to in situ liquid SIMS analysis.

It should be noted that unlike C_{60} or Ar cluster ions, molecular depth profiling of organic thin films using metal cluster primary ions is not feasible because of accumulation of beam damage [34]. Therefore, the self-renewable feature of liquid interfaces (attributable to liquid diffusion and evaporation in many cases) plays an important role to compensate beam damage in in situ liquid SIMS analysis.

Optimization of Beam Current

To further improve the signal intensity, a straightforward consideration is to increase the incident beam current. One option for increasing the beam current is to increase the pulse width. However, the pulse width cannot be too long (≤ 280 ns) because of the ion separation mechanism used in the liquid metal ion gun (See Flash S1 in Supplemental Materials). In addition, though only unit mass resolution is used in this study, a short pulse width is still very helpful for assigning high mass signals ($m/z > 200$). Therefore, increasing pulse width may not be an appropriate choice. It is also possible to reduce cycle time (i.e., increase pulse frequency) to increase the beam current. However, cycle time is proportional to the square root of the measurable mass range due to the time-of-flight principle. Since a reasonable mass range is necessary for in situ SIMS analysis, reducing cycle time may not be a desirable choice in many cases either. Another option to increase the beam current is compromising lateral resolution (increasing beam diameter) of the incident ion beam. Generally speaking, better lateral resolution is a plus for in situ liquid SIMS study because three-dimensional (3-D) distributions of molecular signals are interesting in many cases. However, better signal intensity is normally more desirable.

Increasing the primary ion beam current is helpful in improving signal intensity of the molecular ion, as shown in Figure 3c and d. An interesting observation is that the signal does not increase linearly with beam current. For example, a comparison of Figure 3c with d shows that the m/z 145 signal exhibits ~ 20 times enhancement for only a six times increase in beam current. This situation was commonly observed in all model systems for both negative and positive secondary ions in this research. A plausible explanation is that a stronger beam may create a larger aperture in the SiN membrane, even though the scanned area is kept the same (2 μm in diameter). This explanation is supported by our optical images and SEM images, in which the aperture made by the 200 nm beam is considerably smaller than that made by the 500 nm beam (Supplementary Figure S3).

It should be noted that increasing the beam current may also have some deleterious effects. For example, our previous experience shows that strong beam currents may result in liquid leaking through the aperture and spreading on the high vacuum side of the membrane (shown in Figure 4d), which can ruin the vacuum of the analysis chamber and lead to an automatic shut-

down of the SIMS instrument [14]. The 650 nm Bi^+ , Bi_3^+ , and Bi_3^{++} beams used in this study led to a similar liquid outflow. We found that a 500 nm 0.36 pA Bi_3^+ beam is a good choice for the ionic liquid sample studied here. Under these conditions, a good signal intensity was obtained while limiting the occurrence of unwanted liquid leaking through the aperture to about one case for every 10–20 measurements.

Bi_3^+ or Bi_3^{++}

In agreement with previous reports [28, 30, 35–37], the performances of Bi_3^+ and Bi_3^{++} were found to be similar (for example, Figure 3d and e). Different pulse widths were, however, required to obtain similar currents: 160 ns for the Bi_3^+ beam and 250 ns for the Bi_3^{++} beam at the maximum current. Although only unit-mass resolution can be achieved in our in situ liquid SIMS measurement currently, a narrow pulse width is still desirable because the narrow pulse width can reduce peak overlap (as shown in Figure 3d and e). Therefore, Bi_3^+ is better than Bi_3^{++} for in situ liquid SIMS study.

Aperture Size

One of the unique capabilities of ToF-SIMS is that it can provide 3-D ion images. In acquiring 3-D data, a larger aperture is better because it can provide more spatial information. However, there is a clear tradeoff here that larger aperture size may lead to unwanted leaking of the liquid to the vacuum. The liquid is confined in the aperture because of the liquid's surface

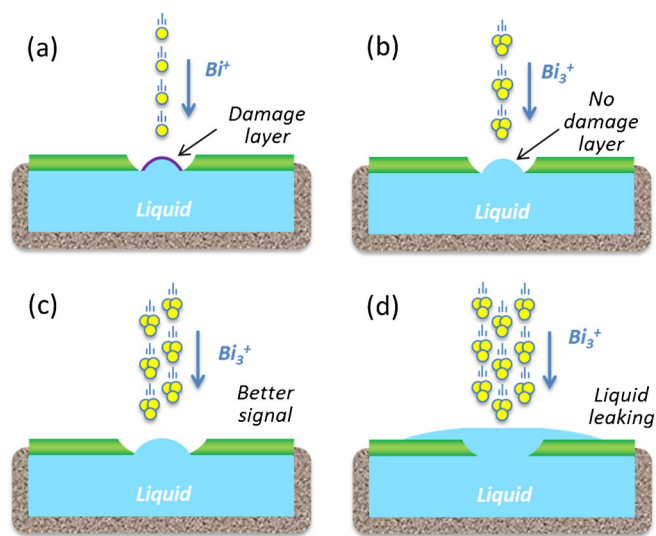


Figure 4. A schematic illustration of optimization of experimental condition for in situ liquid SIMS analysis. **(a)** The monatomic Bi^+ beam leads to a damaged layer at the sputter interface, which diminishes the formation of secondary molecular ions. **(b)** A cluster ion beam (e.g., Bi_3^+) leads to limited beam damage at the sputter interface and molecular ions of reasonable intensity can be detected. **(c)** Better signal intensity can be achieved using an increased incident beam current. **(d)** However, if the incident beam current is too strong or the aperture size is too large, liquid leaks through the aperture, and the vacuum is ruined

tension. Smaller aperture size provides higher holding pressure to confine the liquid in the aperture [12]. If the aperture size becomes larger, surface tension may not be able to confine the liquid within the aperture anymore. Our experimental results show that if we increased the scanned area to 3 μm in diameter, the chance of liquid leaking to the vacuum greatly increased. The practical limit to the scanned area is, therefore, approximately 2 μm in diameter for the ionic liquid sample in this study.

Signal Improvement of Biofilm and Cell Samples

A schematic illustration of the optimization of experimental conditions for in situ liquid SIMS analysis is shown in Figure 4. Based on the previous discussion, a 500 nm 0.36 pA Bi_3^+ beam scanned on an area 2 μm in diameter is recommended for

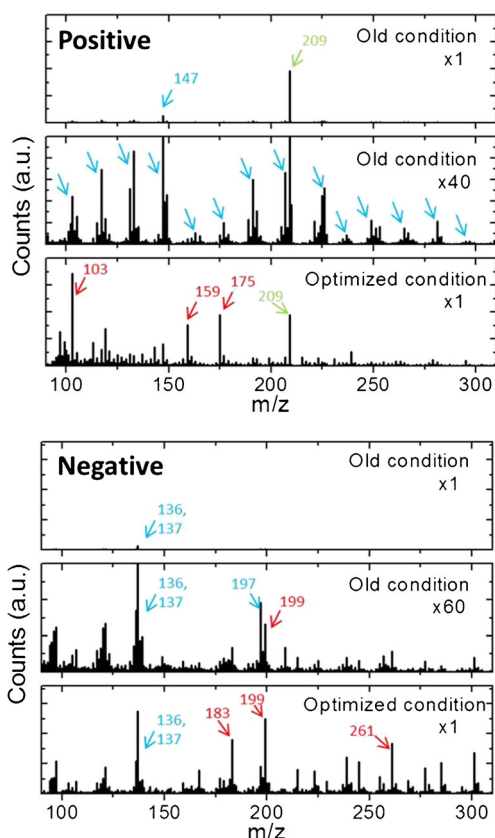


Figure 5. A comparison of positive and negative ion spectra from a live *Shewanella oneidensis* biofilm using optimized condition (a 500 nm 0.36 pA Bi_3^+ beam scanned on an area 2 μm in diameter) and the old condition (a 200 nm 0.20 pA Bi^+ beam scanned on an area 2 μm in diameter) we used in our previous papers [11–17]. The red arrows point to several representative signals from the biofilm, and the peak assignment can be seen in Supplementary Tables S1 and S2. The blue arrows point to the PDMS or Si related signals. For example, in positive ion spectra, the m/z 147 signal, $\text{Si}_2\text{C}_5\text{H}_{15}\text{O}^+$, is a representative signal of PDMS. In negative ion spectra, the m/z 136/137 signals are $\text{Si}_2\text{O}_5^-/\text{Si}_2\text{O}_5\text{H}^-$, and the m/z 197 signal is $\text{Si}_3\text{O}_7\text{H}^-$, all PDMS/ SiO_x characteristic peaks. In addition, the m/z 209 signal in the positive spectra is Bi^+

general in situ liquid SIMS analysis. This condition has been successfully used in our recent biofilm and single cell research [21, 27].

Figure 5 compares the positive and negative ion spectra of a living biofilm sample using a 200 nm 0.20 pA Bi^+ beam (a typical condition used in our initial papers [11–17]) and a 500 nm 0.36 pA Bi_3^+ beam (the optimized condition). For positive secondary ions signals, a 200 nm 0.20 pA Bi^+ beam provided very few useful signals. For example, in the mass range m/z 100–300, only Bi^+ and PDMS-related signals were observed. As a comparison, the 500 nm 0.36 pA Bi_3^+ beam provided a clean spectrum with many useful signals, such as m/z 97, 103, 113, 119, 143, 159, and 175 (peak assignment can be found in Supplementary Tables S1 and S2), and the interference from the PDMS-related signals was not a problem. In addition, all the useful signals were enhanced by at least two orders of magnitude compared with the 200 nm 0.20 pA Bi^+ beam. The negative secondary ion spectrum using the 500 nm 0.36 pA Bi_3^+ beam appeared similar to the negative secondary ion spectrum using the 200 nm 0.20 pA Bi^+ beam. However, the signal intensity of the former also showed a \sim two orders of magnitude improvement. The above observations suggest that the application of the new experimental condition is the key to obtaining useful positive ion spectra in live biofilms. Also, the negative ion data in our previous publications [11–17] are still meaningful, and signal intensity can be greatly improved if the new experimental condition is used.

For cell imaging, characteristic signals from phospholipids are of great interest. Dipalmitoylphosphatidylcholine (DPPC) is one of the phospholipid molecules that has been extensively studied using ToF-SIMS [38–40]. The most characteristic peak of DPPC is the m/z 184 signal, $[\text{C}_5\text{H}_{15}\text{NO}_4\text{P}]^+$, which represents the head group of a DPPC molecule. A positive ion

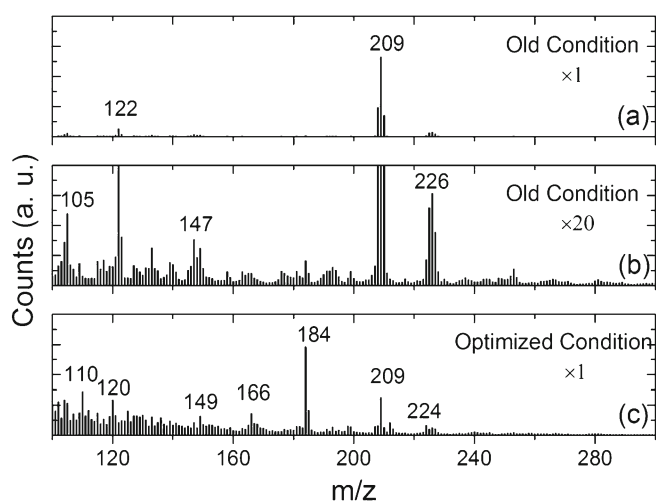


Figure 6. A comparison of positive ion spectra from a C10 cell using the condition (a 200 nm 0.20 pA Bi^+ beam scanned on an area 2 μm in diameter) used in our previous publications [11–17] and the optimized condition (a 500 nm 0.36 pA Bi_3^+ beam scanned on an area 2 μm in diameter). The m/z 184 signal, $[\text{C}_5\text{H}_{15}\text{NO}_4\text{P}]^+$, is a representative signal of DPPC; (a) and (b) old condition; (c) optimized condition

spectrum of hydrated C10 cell using our previous non-optimized beam condition is shown in Figure 6a and b, in which the Bi^+ signal (m/z 209) dominates the mass range of m/z 100–300. Although the m/z 184 signal is observable, it may be too weak to be useful. As a comparison, the spectrum obtained using the optimized condition provides much improved signals of DPPC. Not only does the m/z 184 signal, $[\text{C}_5\text{H}_{15}\text{NO}_4\text{P}]^+$, dominate the spectrum but other characteristic peaks of DPPC, such as m/z 166 ($[\text{C}_5\text{H}_{13}\text{NO}_3\text{P}]^+$) and m/z 224 ($[\text{C}_8\text{H}_{19}\text{NO}_4\text{P}]^+$), are clearly observed. The optimized conditions produced an enhancement of two orders of magnitude in the peak intensity of the m/z 184 signal. Based on the above observation, it is reasonable to conclude that signal intensity of positive secondary ions in in situ liquid SIMS analysis of biological samples is acceptable for further applications.

LiPF₆ EC/DMC Electrolyte

The optimized conditions can also be used to analyze other nonaqueous systems, for example the analysis of a 1.0 M LiPF₆ EC/DMC electrolyte (Supplementary Figure S4). Very strong molecular ion signals are observed because of the ionic character of this sample.

Similar to the other model systems already discussed, beam damage induced by the Bi_3^+ beam was not a problem. In contrast, serious beam damage was observed when the Bi^+ beam was used.

It should be noted that although the optimized conditions recommended here can be used in a variety of non-aqueous systems, there is room for further optimization in specific cases. For example, the liquid leaking through the aperture was more likely to occur when analyzing the LiPF₆ electrolyte. This situation may be attributed to the low surface tension of the organic solvents (EC/DMC). Therefore, the SIMS conditions may need to be tuned accordingly for different liquids using the principles outlined here.

Mass Resolution

As mentioned before, only unit mass resolution can be achieved because high spatial resolution mode is used in in situ liquid SIMS analysis. The detailed reason why high mass resolution and high spatial resolution cannot be achieved simultaneously in a traditional ToF-SIMS instrument is described in Flash S2 in Supplementary Materials. The low mass resolution may be the next challenge for extending applications of in situ liquid SIMS. Recently, several new ToF-SIMS instrumentations have been developed that can simultaneously provide high mass resolution and high spatial resolution with reasonable signal intensity. Two examples are the J105 from IONOPTIKA [41] and the attachment of an Orbitrap on a ToF-SIMS [42]. The combination of in situ liquid SIMS with these instrumental advances will be ideal for investigation of liquid interfaces at the molecular level.

Conclusions

In situ liquid SIMS is a promising new technique. However, the initial results suffered from the low signal intensity for molecular and characteristic fragment ion species, especially in the positive ion mode. In this study, we used four model systems to optimize the experimental conditions, and successfully improved signal intensities for both positive and negative characteristic secondary ions. A 500 nm 0.36 pA Bi_3^+ beam (25 kV) scanned on an area 2 μm in diameter is recommended for general in situ liquid SIMS analysis. Beam damage induced by the 25 keV Bi_3^+ beam is not problematic for in situ liquid SIMS measurement despite the high ion doses that are two to four orders of magnitude higher than the static limit. The signal intensities of molecular ions and characteristic fragment ions improve by about two orders of magnitude compared with our initial 200 nm Bi^+ beam. The optimized condition can be used to study various aqueous or nonaqueous liquid samples, although there may be room for further improvement because of variations of surface tensions among different liquids. This study provides a reliable set of conditions to investigate liquid interfaces using in situ liquid SIMS.

Acknowledgments

This work was funded by Laboratory Directed Research and Development (LDRD) programs of the Pacific Northwest National Laboratory (PNNL), which include an FY16 Open Call LDRD, an EBSD FY16 Seed LDRD, and an MS³ LDRD. The work was performed at EMSL, a national scientific user facility sponsored by the Department of Energy's Office of Biological and Environmental Research located at PNNL. We also appreciate Mr. Decarle Jin for his English editing.

References

- Beech, I.B., Smith, J.R., Steele, A.A., Penegar, I., Campbell, S.A.: The use of atomic force microscopy for studying interactions of bacterial biofilms with surfaces. *Colloid Surface B* **23**, 231–247 (2002)
- Wright, C.J., Shah, M.K., Powell, L.C., Armstrong, I.: Application of AFM From Microbial Cell to Biofilm. *Scanning* **32**, 134–149 (2010)
- Schaudinn, C., Carr, G., Gorur, A., Jaramillo, D., Costerton, J.W., Webster, P.: Imaging of endodontic biofilms by combined microscopy (FISH/cLSM - SEM). *J. Microsc. Oxford* **235**, 124–127 (2009)
- Oubekka, S.D., Briandet, R., Fontaine-Aupart, M.P., Steenkeste, K.: Correlative time-resolved fluorescence microscopy to assess antibiotic diffusion-reaction in biofilms. *Antimicrob. Agents Chemother.* **56**, 3349–3358 (2012)
- Chao, Y.Q., Zhang, T.: Surface-enhanced Raman scattering (SERS) revealing chemical variation during biofilm formation: from initial attachment to mature biofilm. *Anal. Bioanal. Chem.* **404**, 1465–1475 (2012)
- Nichols, P.D., Henson, J.M., Guckert, J.B., Nivens, D.E., White, D.C.: Fourier transform-infrared spectroscopic methods for microbial ecology—analysis of bacteria, bacteria-polymer mixtures, and biofilms. *J. Microbiol. Method* **4**, 79–94 (1985)
- Nivens, D.E., Chambers, J.Q., Anderson, T.R., Tunlid, A., Smit, J., White, D.C.: Monitoring microbial adhesion and biofilm formation by attenuated total reflection Fourier-transform infrared-spectroscopy. *J. Microbiol. Method* **17**, 199–213 (1993)
- Abadian, P.N., Tandogan, N., Jamieson, J.J., Goluch, E.D.: Using surface plasmon resonance imaging to study bacterial biofilms. *Biomicrofluidics* **8**, 021804 (2014)

9. Benninghoven, A.: Chemical analysis of inorganic and organic surfaces and thin films by static time-of-flight secondary ion mass spectrometry (TOF-SIMS). *Angew. Chem., Int. Ed.* **33**, 1023–1043 (1994)
10. Wirtz, T., Philipp, P., Audinot, J.N., Dowsett, D., Eswara, S.: High-resolution high-sensitivity elemental imaging by secondary ion mass spectrometry: from traditional 2-D and 3-D imaging to correlative microscopy. *Nanotechnology* **26**, 434001 (2015)
11. Yang, L., Yu, X.Y., Zhu, Z.H., Iedema, M.J., Cowin, J.P.: Probing liquid surfaces under vacuum using SEM and ToF-SIMS. *Lab Chip* **11**, 2481–2484 (2011)
12. Yang, L., Yu, X.Y., Zhu, Z.H., Thevuthasan, T., Cowin, J.P.: Making a hybrid microfluidic platform compatible for in situ imaging by vacuum-based techniques. *J. Vac. Sci. Technol. A* **29**, 061101 (2011)
13. Yang, L., Zhu, Z.H., Yu, X.Y., Rodek, E., Saraf, L., Thevuthasan, T., Cowin, J.P.: In situ SEM and ToF-SIMS analysis of IgG conjugated gold nanoparticles at aqueous surfaces. *Surf. Interface Anal.* **46**, 224–228 (2014)
14. Yang, L., Zhu, Z.H., Yu, X.Y., Thevuthasan, S., Cowin, J.P.: Performance of a microfluidic device for in situ ToF-SIMS analysis of selected organic molecules at aqueous surfaces. *Anal. Methods UK* **5**, 2515–2522 (2013)
15. Liu, B.W., Yu, X.Y., Zhu, Z.H., Hua, X., Yang, L., Wang, Z.Y.: In situ chemical probing of the electrode-electrolyte interface by ToF-SIMS. *Lab Chip* **14**, 855–859 (2014)
16. Hua, X., Yu, X.Y., Wang, Z.Y., Yang, L., Liu, B.W., Zhu, Z.H., Tucker, A.E., Chrisler, W.B., Hill, E.A., Thevuthasan, T., Lin, Y.H., Liu, S.Q., Marshall, M.J.: In situ molecular imaging of a hydrated biofilm in a microfluidic reactor by ToF-SIMS. *Analyst* **139**, 1609–1613 (2014)
17. Hua, X., Marshall, M.J., Xiong, Y.J., Ma, X., Zhou, Y.F., Tucker, A.E., Zhu, Z.H., Liu, S.Q., Yu, X.Y.: Two-dimensional and three-dimensional dynamic imaging of live biofilms in a microchannel by time-of-flight secondary ion mass spectrometry. *Biomicrofluidics* **9**, 031101 (2015)
18. Zhu, Z.H., Zhou, Y.F., Yan, P.F., Vemuri, R.S., Xu, W., Zhao, R., Wang, X.L., Thevuthasan, S., Baer, D.R., Wang, C.M.: In situ mass spectrometric determination of molecular structural evolution at the solid electrolyte interphase in lithium-ion batteries. *Nano Lett.* **15**, 6170–6176 (2015)
19. Yu, J., Zhou, Y., Hua, X., Liu, S.Q., Zhu, Z.H., Yu, X.Y.: Capturing the transient species at the electrode-electrolyte interface by in situ dynamic molecular imaging. *Chem. Commun* **52**, 10952–10955 (2016)
20. Jessop, P.G., Heldebrant, D.J., Li, X.W., Eckert, C.A., Liotta, C.L.: Green chemistry—reversible nonpolar-to-polar solvent. *Nature* **436**, 1102–1102 (2005)
21. Ding, Y.Z., Zhou, Y.F., Yao, J., Szymanski, C., Shi, L., Cao, B., Zhu, Z.H., Yu, X.Y.: Imaging *Shewanella oneidensis* biofilm matrix by in situ liquid ToF-SIMS. *Anal. Chem.* Submitted, (2016)
22. Yu, J.C., Zhou, Y.F., Hua, X., Zhu, Z.H., Yu, X.Y.: In situ characterization of hydrated proteins in water by SALVI and ToF-SIMS. *J. Vis. Exp.* **108**, e53708 (2016)
23. Shen, K., Tarolli, J.G., Winograd, N.: Cluster secondary ion mass spectrometry imaging of interfacial reactions of TiO₂ microspheres embedded in ionic liquids. *Rapid Commun. Mass Spectrom.* **30**, 379–385 (2016)
24. Liu, Y., Lu, C.Y., Twigg, S., Ghaffari, M., Lin, J.H., Winograd, N., Zhang, Q.M.: Direct observation of ion distributions near electrodes in ionic polymer actuators containing ionic liquids. *Sci. Rep. UK* **3**, 973 (2013)
25. Dertinger, J.J., Walker, A.V.: Ionic liquid matrix-enhanced secondary ion mass spectrometry: the role of proton transfer. *J. Am. Soc. Mass Spectrom.* **24**, 348–355 (2013)
26. Fitzgerald, J.J.D., Kunnath, P., Walker, A.V.: Matrix-enhanced secondary ion mass spectrometry (ME SIMS) using room temperature ionic liquid matrices. *Anal. Chem.* **82**, 4413–4419 (2010)
27. Hua, X., Szymanski, C., Wang, Z.Y., Zhou, Y.F., Ma, X., Yu, J.C., Evans, J.E., Orr, G., Liu, S.Q., Zhu, Z.H., Yu, X.Y.: Correlative chemical imaging of hydrated single cells by secondary ion mass spectrometry and super-resolution microscopy. *Integr. Biol.* **8**, 635–644 (2016)
28. Kollmer, F.: Cluster primary ion bombardment of organic materials. *Appl. Surf. Sci.* **231/232**, 153–158 (2004)
29. Touboul, D., Kollmer, F., Niehuis, E., Brunelle, A., Laprevote, O.: Improvement of biological time-of-flight-secondary ion mass spectrometry imaging with a bismuth cluster ion source. *J. Am. Soc. Mass Spectrom.* **16**, 1608–1618 (2005)
30. Zhu, Z.H., Shutthanandan, V.: Are cluster ion analysis beams good choices for hydrogen depth profiling using time-of-flight secondary ion mass spectrometry? *Surf. Interface Anal.* **44**, 89–93 (2012)
31. Szakal, C., Kozole, J., Russo, M.F., Garrison, B.J., Winograd, N.: Surface sensitivity in cluster-ion-induced sputtering. *Phys. Rev. Lett.* **96**, 216104 (2006)
32. Szakal, C., Kozole, J., Winograd, N.: Fundamental studies of the cluster ion bombardment of water ice. *Appl. Surf. Sci.* **252**, 6526–6528 (2006)
33. Cheng, J., Wucher, A., Winograd, N.: Molecular depth profiling with cluster ion beams. *J. Phys. Chem. B* **110**, 8329–8336 (2006)
34. Cheng, J., Kozole, J., Hengstebeck, R., Winograd, N.: Direct comparison of Au-3(+) and C-60(+) cluster projectiles in SIMS molecular depth profiling. *J. Am. Soc. Mass Spectrom.* **18**, 406–412 (2007)
35. Russo, M.F., Szakal, C., Kozole, J., Winograd, N., Garrison, B.J.: Sputtering yields for C-60 and Au-3 bombardment of water ice as a function of incident kinetic energy. *Anal. Chem.* **79**, 4493–4498 (2007)
36. Zhu, Z.H., Nachimuthu, P., Lea, A.S.: Molecular depth profiling of sucrose films: a comparative study of C-60(n+) ions and traditional Cs+ and O-2(+) ions. *Anal. Chem.* **81**, 8272–8279 (2009)
37. Nagy, G., Lu, P., Walker, A.V.: An investigation of secondary ion yield enhancement using Bi-n(2+) (n=1, 3, 5) primary ions. *J. Am. Soc. Mass Spectrom.* **19**, 33–45 (2008)
38. Cannon, D.M., Pacholski, M.L., Winograd, N., Ewing, A.G.: Molecule specific imaging of freeze-fractured, frozen-hydrated model membrane systems using mass spectrometry. *J. Am. Chem. Soc.* **122**, 603–610 (2000)
39. Ostrowski, S.G., Van Bell, C.T., Winograd, N., Ewing, A.G.: Mass spectrometric imaging of highly curved membranes during *Tetrahymena* mating. *Science* **305**, 71–73 (2004)
40. Kurczy, M.E., Piehowski, P.D., Van Bell, C.T., Heien, M.L., Winograd, N., Ewing, A.G.: Mass spectrometry imaging of mating *Tetrahymena* show that changes in cell morphology regulate lipid domain formation. *Proc. Natl. Acad. Sci. U.S.A.* **107**, 2751–2756 (2010)
41. Rabbani, S., Fletcher, J.S., Lockyer, N.P., Vickerman, J.C.: Exploring subcellular imaging on the buncher-ToF J105 3D chemical imager. *Surf. Interface Anal.* **43**, 380–384 (2011)
42. Available atL <https://www.iontof.com/news-ion-tof-sims-events.html>; accessed March 11, (2016)